

# DETONATION COMBUSTION OF A GAS MIXTURE IN A CYLINDRICAL CHAMBER

F. A. Bykovskii and V. V. Mitrofanov

Voitsekhovskii [1, 2] was the first to propose and realize a method of continuous combustion of a gas mixture in transverse detonation waves, circulating in a toroidal chamber. The combustion chamber used was a planar circular channel in which fuel supply and product exhaust were accomplished in a radial direction through interior and exterior slits. The velocity of the transverse detonation waves along the channel in these experiments was close to the speed of sound in the reaction products. The wave structure was not described [3]. Fairly recently, detonation combustion regimes have been achieved in a ring chamber of circular geometry with a structure recalling conventional spin detonation in a circular tube, and a number of principles governing the process have been clarified [4]. The present study will present more detailed results of a study of this phenomenon.

## Experimental Technique

The experimental chamber (Fig. 1) was a Plexiglas cylinder, closed at the top, with diameter  $d_c = 40$  mm and length  $L = 100$  mm, with interchangeable axial inserts. A quartz tube (wall thickness 2-3 mm) was installed within the cylinder for thermal protection. The gaseous components were supplied individually through two series of orifices in the cap closing the upper end of the cylinder. In all the experiments oxygen was used as the oxidizer, while acetylene, methane, propane, and hydrogen were used as the fuel. The oxygen and fuel gas were supplied to the chamber from reservoirs through high-speed electromagnetic valves. The mixture was controlled by the pressure in the reservoirs and the total area of the inlet orifices. In the experiments described below, if no special note is made of the excess fuel coefficient  $\Phi$ , the mixture was close to stoichiometric.

Detonation was initiated 0.1 sec after opening the valves by a high-voltage discharge with energy of about 10 J within a special channel, located at the chamber wall or in the central insert (tangent to the interior surface) 35 mm from the cylinder cap. The mixture flowed freely into this channel after admission to the chamber. Upon exiting the channel into the gap the detonation wave produced transverse detonation waves in a definite direction. In the majority of the experiments the entire process lasted 0.3 sec and was terminated automatically by closing of the valves.

The detonation products were exhausted into a special chamber about  $0.5 \text{ m}^3$  in volume, from which air and the exhaust gases of the previous experiment had been removed to a pressure of 20 mm Hg. The lower face of the chamber was connected to the vacuum volume by a section of tube 200 mm long with diameter of 54 mm.

The process within the chamber was recorded photographically through a vertical or horizontal slit, on a film moving perpendicular to the slit (camera axis situated vertically). The number of waves and their

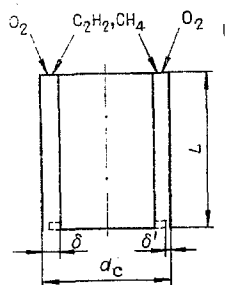


Fig. 1. Axial section of the chamber.

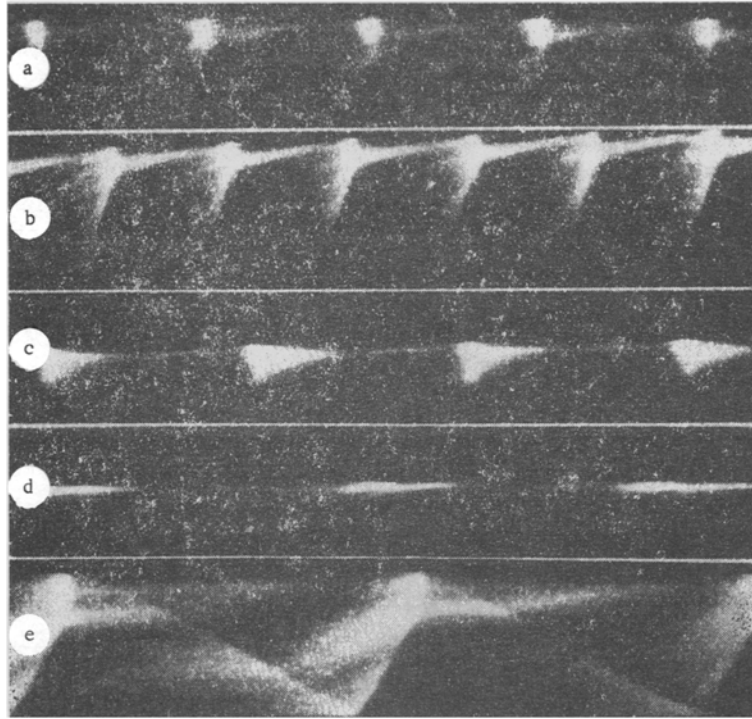


Fig. 2. Photoregistrogram of process in cylindrical ring chamber with acetylene-oxygen (a-d) and methane-oxygen (e) mixtures. a)  $\Phi = 0.9$ ,  $\delta = \delta' = 2.5$  mm,  $L = 20$  mm,  $D = 1600$  m/sec,  $n = 3$ ; b)  $\Phi = 4.0$ ,  $\delta = \delta' = 5$  mm,  $L = 85$  mm,  $D = 2000$  m/sec,  $n = 2$ ; c)  $\Phi = 1.0$ ,  $\delta = \delta' = 5$  mm,  $L = 85$  mm,  $D = 1620$  m/sec,  $n = 2$ ; d)  $\Phi = 0.63$ ,  $\delta = \delta' = 1.25$  mm,  $L = 85$  mm,  $D = 770$  m/sec,  $n = 2$ ; e)  $\Phi = 1.0$ ,  $\delta = 5.0$  mm,  $\delta' = 2.5$  mm,  $L = 45$  mm,  $D = 1890$  m/sec,  $n = 1$ .

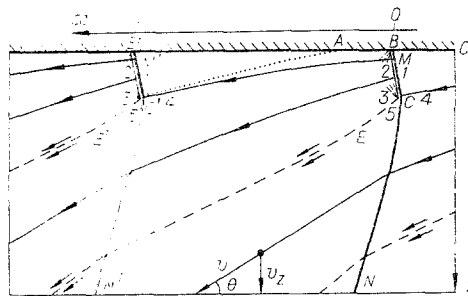


Fig. 3. Flow pattern.

velocity were determined from photographs taken through a horizontal slit located near the chamber cap. To expose the fine structure of the flow, photography was performed through a vertical slit using the full compensation method [5], i.e., the film speed was maintained equal to the speed of the wave image. Thus in the steady-state regime the photographic image corresponded exactly to the corresponding instantaneous brightness distribution in the wave. Compensation method photography through a vertical slit 10 mm wide permitted monitoring of the velocity and number of waves in each experiment by measuring the distance between successive images on the film. A number of the experiments used a chamber similar in principle to that of Fig. 1, but with a rectangular cross section.

#### Flow Structure. Range of Regime Existence

Transverse detonation waves burning up the gas mixture were obtained in the chamber described over a quite wide range of experimental conditions. Several photographs of such waves in the steady-state regime are presented in Fig. 2a-c, while corresponding flow patterns are shown in Fig. 3.

The transverse detonation wave BC moves within region 1, which contains unreacted fuel which has entered through the chamber end wall. Behind the wave the production products expand gradually and are driven downward by new quantities of the gases entering in the segment AB' (in the segment BA draft ceases because of high counterpressure). Conditions are created for propagation of the following transverse detonation wave (if the wave number  $n > 1$ ), or of the same wave in a subsequent cycle (if  $n = 1$ ). The number of waves is established spontaneously, with four being achieved in the acetylene-oxygen mixture. In the experiments with the methane-oxygen mixture in this chamber only regimes with  $n = 1$  were obtained. From below each transverse detonation wave there departs an oblique shock wave CN, moving through the detonation products. This wave is analogous to the tail of spin combustion in tubes, but is more inclined to the rear. In the methane-oxygen mixture the wave CN glows more brightly than in the stoichiometric acetylene-oxygen mixture, as in conventional detonation in tubes. In a very rich acetylene mixture the brightness of the oblique wave intensifies (see Fig. 2b), probably because of the appearance of free carbon in the detonation products.

In the propane-oxygen mixture transverse waves were excited just as easily as in the acetylene and methane mixtures. In the hydrogen-oxygen mixture photographs could not be obtained because of the low brightness level produced by the reaction.

The similarity of certain of the photographs in the acetylene-oxygen mixture (Fig. 2c) to ones obtained previously [1-3] in a planar ring channel is interesting. Apparently the flow pattern with reflected oblique inflammation wave proposed in [5] to explain the brightness pattern does not correspond to reality. It is more realistic to treat the phenomenon observed on the basis of the pattern shown in Fig. 3; the major portion of the radiating triangle with small angle directed forward is most probably, just as in our experiments, the region of the original mixture AB'C', burning from the lower surface due to contact with an underlying layer of reaction products, while a transverse discontinuity (B'C') is located ahead of the slightly inclined back side of the triangle and is not always distinguishable against the background of the triangle's bright radiation. Rapid burnup of the mixture behind the transverse discontinuity leads to cessation of radiation at the back side of the triangle. Such an assumption agrees with the peaks in pressure determined in this region [3]. The breakaway of the glowing triangle from the inner edge of the ring channel observed in [3] can be explained by delays in inflammation of the original mixture.

The effect of the geometrical parameters  $\delta$  and L (Fig. 1) on the detonation combustion regime is shown by Table 1. The methane supply pressure was varied over the range 5-8 atm, which corresponds to a flow rate into the chamber  $G_T = 6.4-10$  g/sec and a mean pressure in the chamber near the cap  $p_C = 1-1.6$  atm for  $\delta = 5$  mm. To ensure stoichiometry of the mixture, the oxygen supply pressure was  $\approx 1.5$  times higher. The acetylene supply pressure was varied from 0.7 to 2.1 atm, corresponding to  $G_T = 1.3-3.9$  g/sec and  $p_C = 0.33-1$  atm at  $\delta = 2.5$  mm. As is evident from Table 1, there is a certain lower critical gap width  $\delta_{min}$ , such that at  $\delta < \delta_{min}$  within the ranges of the other parameters used in the study, transverse detonation waves could not be excited. For the mixture  $CH_4-O_2$   $\delta_{min} \approx 2.5$  mm, for  $C_2H_2-O_2$   $1.25 < \delta < 2.5$  mm. In the mixture  $CH_2H_2-O_2$  at  $\delta = 1.25$  mm and L = 17 mm only conventional combustion develops, while at L = 85 mm a "beaded" structure

TABLE 1

$\delta$ , mm	L, mm	$G_T$ , g/sec	n	D, km/sec
$CH_4-O_2$				
2.5 *	85	7.5	1	—
		10.0	2	—
5	85	8	1	1.6
	40	8	1	1.9
$C_2H_2-O_2$				
2.5	85	3.9	4	1.8
		2.8	3	1.9
		1.9	2	1.6
	40	3.9	3	2.1
		3.1	3	2.0
		1.6	2	1.7
20	2.3	2	1.6	
		2	1.6	
5.0	85	3.9	2	2.4
		1.3	2	1.6

\* Nonstationary process.

was occasionally observed in the flowing zone, as shown in Fig. 2d. Here the process is greatly affected by the hydrodynamic resistance of the channel to the exciting products. A marked reduction in gas flow rate at the same reservoir pressure indicated departure from the critical exhaust to the chamber regime.

In the general case, the value of  $\delta_{\min}$  should depend both on the chemical properties of the mixture and the value of the pressure in the chamber  $p_1$  and on the geometric parameters of the gas mixing zone near the cap. Estimation of  $p_1$  ahead of the wave shows that it is approximately two times lower than the  $p_c$  values given above. At such pressures the critical detonation diameter in a smooth tube, estimated from the mean size of the detonation cell, comprises 3-2 mm and 0.6-0.2 mm for the mixtures under consideration. Since for acetylene  $\delta_{\min}$  proves to be several times larger than  $d_{cr}$ , it can be assumed that in this case  $\delta_{\min}$  depends on the mixing rate. For methane  $\delta_{\min}/d_{cr} \approx 1$  and  $\delta_{\min}$  here is most probably limited by the chemical reaction time, i.e., is of the same nature as  $d_{cr}$  of premixed mixtures in smooth tubes.

At  $\delta = 2.5$  mm in the methane-oxygen mixture transverse detonation waves are unstable: A structure like that of Fig. 2b was observed for 1-3 cycles, then disappeared and was reestablished after several cycles. A stable stationary process occurred at  $\delta = 2.5$  mm in the acetylene-oxygen mixture and at  $\delta = 5$  mm in both mixtures.

The wave velocity increases with increase in  $\delta$ , with decrease in chamber length within certain limits, and with increase in fuel flow, while  $n$  remains unchanged. At  $L = 40$  mm the most stable regime develops with a velocity approaching that of ideal Chapman-Jouguet detonation.

The detonation combustion process was maintained when a rectangular ring was installed on the insert, narrowing the exit from the ring channel to some value  $\delta' < \delta$ . Ring installation did, however, lead to a change in the transverse detonation wave parameters and the character of flow in the chamber. Reflection of the shock wave in the combusted products developed. In the  $\text{CH}_4\text{-O}_2$  mixture at  $\delta = 5$  mm,  $\delta' = 2.5$  mm, and  $L = 45$  mm the reflected wave reached the face of the chamber at approximately the same time as the detonation wave from the following cycle, encouraging stabilization of the process (a resonant phenomenon, see Fig. 2e). At  $L = 80$  mm with other parameters maintained the same, the reflected wave reaches the upper face of the chamber at a point removed from the transverse detonation wave of the following cycle by approximately half a period. In the region of repeated reflection from the upper face, a new chemical reaction hearth developed in the fresh mixture, which periodically changes into a new detonation wave. The development of the new wave leads to attenuation of the first one, because of burnup of fresh mixture ahead of the first wave. Because of these phenomena, a process is established with two unstable waves, each of which periodically intensifies and attenuates, leading to simultaneous changes in the distance between the waves.

Narrowing of the gap at the chamber output by a factor of four ( $\delta' = 1.25$  mm for  $\delta = 5$  mm) leads to extinction of the detonation waves in the methane-oxygen mixture with their conversion into acoustic waves; conventional combustion is maintained in the chamber, intensified at points of reflection of the inclined acoustic waves from the upper surface of the chamber. Photographs of this process are shown in Fig. 2e, and are marked by the absence of a bend in the oblique wave in the region of reflection from the upper face. An interesting peculiarity of the process is the absence of purely longitudinal or transverse modes of acoustic oscillation and the development of a single longitudinal-transverse mode in the form of a closed system of oblique waves traveling through the ring gap in one direction. Each subsequent wave in such a system is a reflection of one of the preceding waves, and because of the closed nature of the channel all waves are "subsequent" ones. The process of Fig. 2e has a similar wave pattern, but is distinguished by the presence of transverse detonation waves near the chamber top, in which combustion of a significant portion of the fresh mixture is localized. The existence of these waves is not necessarily related to reflection of a preceding wave.

In the acetylene-oxygen mixture, even upon narrowing of the output channel by a factor of two ( $\delta = 2.5$  mm,  $\delta' = 1.25$  mm,  $L = 35$  mm) transverse detonation waves with a normal structure disappear and the photographs show a beaded brightness pattern similar to that of Fig. 2d. The rotation rate of the glowing region ( $n = 1$ ) is about 1500 m/sec, i.e., supersonic. The most probable explanation of this phenomenon is that the radiation is produced by intensified combustion of the mixture near the upper chamber face by oblique acoustic waves described above, since the peripheral phase velocity is supersonic. However, in contrast to the methane-oxygen mixture, no oblique waves were recorded on the photographic film. This could be explained by their low brightness level as compared to the mixture combustion zone. Upon narrowing of the section by a factor of 2.5 ( $\delta = 2.5$  mm,  $\delta' = 1$  mm,  $L = 18$  mm) unstable combustion filling the entire chamber volume was observed.

Experiments on detonation combustion were also performed in a rectangular chamber with cross section of  $40 \times 5$  mm and in a circular chamber with a full barrier directed parallel to the chamber axis. The barriers (one or two) eliminated stationary rotary wave motion in one direction, producing waves traveling toward each other because of reflections, i.e., in this case the geometric conditions in the rectangular and circular chambers were similar. It was assumed that a process of combustion in a system of periodically colliding oppositely directed waves could be produced, similar to that behind a moving detonation front in planar rectangular channels [5].

In the acetylene-oxygen mixture a process was observed with several oppositely directed waves, periodically reflecting from each other or the side walls or barriers. As fuel flow was reduced two oppositely directed waves remained, being replaced with further reduction by a single wave reflecting from the chamber walls. The mean wave velocity in the transverse direction for the acetylene-oxygen mixture in both chambers was close to the speed of sound in the combustion products ( $D=1250-1000$  m/sec), which confirms the analogy to processes behind a traveling multifront detonation wave. However, a characteristic feature of these regimes was the strong irregularity of the transverse wave motion, and the absence within the waves of any ordered structure, comparable to the transverse wave structure in conventional detonation in planar channels. Evidently, the absence of a forward pulsating shock front igniting about half the mixture [6] in the high speed stage of motion has a destabilizing effect in this instance. A significant portion of the fuel here combusts by a conventional burning mechanism and the length of the reaction zone is longer than in the case of transverse detonation waves continuously circulating around the periphery of the circular channel. This is shown by the more homogeneous distribution of brightness over chamber length. In experiments with methane only one transverse wave was excited, moving between the reflecting walls with a mean velocity below 800 m/sec, but not damping over the course of the entire process. It can be assumed that the lower velocity is related to incomplete combustion.

Thus, although it was possible to create a combustion regime in the chamber with oppositely directed waves, similar to that occurring behind the forward shock front of multifront (pulsating) detonation, on the whole we can conclude that a chamber geometry not completely closed into a ring has a negative effect on detonation combustion: The mean transverse wave velocity falls sharply, the wave structure becomes diffuse, stability is lost, and combustion time is lengthened.

At the same time, in the ring chamber without barriers, regimes with stable transverse waves in one direction of rotation were excited over a relatively wide range of conditions, producing continuous combustion of the gas mixture in a narrow zone near the chamber cap. The size of this zone in the axial direction is determined by the dimensions of the wave front just as in the regular cellular structure of a detonation front in planar channels [5, 6].

Additional data on propane detonation combustion regimes in a ring chamber having a narrow nozzle gap can be found in [7]. In that study the wave structure was not resolved optically, but pressure profiles were measured, showing an increase of 10-15 times at the discontinuity. The velocity of wave motion agrees well with the data on the chamber with narrowed output.

#### Analysis of Flow in Constant Section Chamber

Considering the flow in the annular chamber space to be two-dimensional and stationary with respect to the transverse detonation waves, we use the flow pattern depicted in Fig. 3 and corresponding experimental data for the chamber with no narrowing of the output section. The coordinate  $x$  is measured along the mean chamber circumference. The flow in this case is analogous to that which has been studied near waves in spin and multifront detonation of gases in long tubes and channels [5]. The major difference is the replacement of the primary shock discontinuity by the planar end face of the chamber, through which the mixture components are supplied. Here the necessity of complicating the pattern by ternary shock and shock-detonation configurations is absent. Although the appearance of a forward projecting "nose" at the upper edge of the transverse waves, characteristic of spin detonation, was recorded in some photographs [4], it is not an obligatory phenomenon in this case and can easily be eliminated by adjustments in construction. The ternary shock configuration at the lower edge of the transverse waves occurring in the flow pattern of [4] and also recorded experimentally herein was studied in greater detail and found to occur under conditions of restricted exhaust from the chamber: either with small  $\delta$  and large  $L$ , where braking in the boundary layer on the walls is significant, or in the presence of a narrowed outlet from the chamber ring.

With free exhaust of the products from the open end of the chamber, which will be analyzed here, the observed discontinuity CN in the upper part of the chamber is either approximately vertical or inclined slightly

to the rear (leftward), as in Fig. 3. With growth in  $z$  its inclination increases, with intensity decreasing correspondingly. Adjustment of the flow behind the transverse wave and the wave CN in the vicinity of the conjugate point C occurs through a centralized rarefaction wave. The initial slope of the discontinuity CN is calculated from the condition of equality of pressure and flow direction along the contact discontinuity CE. The second rarefaction wave, beginning at point B, is necessary to reconcile the flow behind the transverse wave with conditions at the wall.

We will assume heat loss at the walls and friction to be negligible, with the state of the mixture ahead of and directly behind the transverse wave being homogeneous along the wave front. We further assume the entire gas to be ideal, with constant heat capacity ratio  $\gamma$ , that the chemical reaction is frozen at all points behind the wave, that the flow at large  $z$  is homogeneous, and that the exhaust velocity at the chamber section is sonic:

$$v_z = c. \quad (1)$$

We will assume the transverse detonation wave to be a self-maintaining Chapman-Jouguet wave with instantaneous chemical reaction in the plane front.

These assumptions permit writing a first group of equations, relating the flow parameters in regions 1 and 2 (see Fig. 3) in the form of known relationships on the detonation front:

$$\begin{aligned} \rho_1 v_1 &= \rho_2 v_2, \\ p_1 + \rho_1 v_1^2 &= p_2 + \rho_2 v_2^2, \\ p_2 &= \frac{1}{\gamma} \rho_2 v_2^2, \\ I_1 + \frac{v_1^2}{2} &= \frac{\gamma + 1}{\gamma - 1} \frac{v_2^2}{2}, \\ I_1 &= \frac{\gamma}{\gamma - 1} \frac{p_1}{\rho_1} + H_1, \quad \theta_1 = \theta_2. \end{aligned} \quad (2)$$

The enthalpy  $I_1$  includes the heat of formation of the mixture components  $H_1$ , with reference level chosen so that in the state behind the wave  $H_2 = 0$ , and  $\theta$  is the angle of inclination of the flow lines to the  $x$  axis.

Region 2 behind the wave, where  $v_2 = c_2$  in view of the Chapman-Jouguet condition, is the critical one for the stationary regime under consideration. The pressure  $p_2$  is maximum with respect to all remaining points of the flow, and the flow outside region 2 is supersonic everywhere relative to the transverse detonation wave. Exceptions are the inner region (chempeak region), which will not be analyzed, and possibly the small region 5 behind the oblique shock wave CN in the vicinity of the point C. The medium ahead of the transverse wave is a mixture of fuel and oxidizer, the products of their possible combustion, and also the detonation products behind the preceding wave, which latter dilute the mixture, reducing  $H_1$ .

Due to flow expansion behind the wave, products can arrive in region 1 only from the upper zone of the preceding wave, denoted arbitrarily in Fig. 3 by the flow line MC'. The fraction of the mass flux through this zone as compared to the total mass flux will be denoted by  $\kappa$ . In view of the periodicity of the process, this fraction can be considered as continually circulating in the transverse zone, and it enters into the total mass flux through the transverse zone, but does not appear in the fuel flow rate  $G$  entering the chamber in the  $z$  direction. The fuel flow rate  $G_1$  for a single wave is then equal to the other part of the mass of material which passes through the wave below the flow line MC' per unit time:

$$G_1 = (1 - \kappa) h \delta \rho_1 v_1 = h_1 \delta \rho_2 v_2. \quad (3)$$

Here  $h$  is the size of the wave;  $h_1 = (1 - \kappa)h$ .

Along this boundary flow line MC', the form of which is unknown in the general case, there occurs an interaction of the flow entering the wave with the "pure" detonation products of the preceding wave located below the flow. We introduce a notation of mean pressure forces acting between these flows in the corresponding directions, together with their ratio:

$$\begin{aligned} p_z &= \frac{1}{l - h_1 \sin \theta_1} \int_{MC'} p(x, z) dx, \\ p_x &= \frac{1}{h_1 \cos \theta_1} \int_{MC'} p(x, z) dz, \quad \alpha = \frac{p_x}{p_z}, \end{aligned} \quad (4)$$

where integration is performed along the flow line MC' between two neighboring waves. Then from the equations for the projections of momentum on the  $x$  and  $z$  axes, after transformations we obtain

$$\frac{D}{v_2} = \left[ \frac{(\gamma+1)}{\gamma} - \frac{1}{\gamma} \frac{p_x}{p_2} \right] \cos \theta_1 - \frac{\bar{u}_{0x}}{v_2},$$

$$\frac{p_c}{p_2} + \gamma \frac{\bar{u}_z}{v_2} \frac{h_1}{l} = (\gamma+1) \frac{h_1}{l} \sin \theta_1 + \left( 1 - \frac{h_1}{l} \sin \theta_1 \right) \frac{p_2}{p_c}, \quad (5)$$

where  $\bar{u}_{0x}$  and  $\bar{u}_{0z}$  are the projections of the mean velocity of the original gases when drafted into the chamber.

To find the projection of the mixture velocity relative to the walls ahead of the wave  $u_{1x}$ , we use the kinematic equation

$$D + u_{1x} = v_1 \cos \theta_1,$$

from which after dividing by  $v_2$  and using Eqs. (5) and (2) we find

$$(u_{1x} - \bar{u}_{0x})/v_2 = (p_x - p_1)/\gamma p_2 \cdot \cos \theta_1. \quad (6)$$

With regard to the energy relationship between the initial state of the gases and the state behind the wave, it is necessary to consider the work of reaction forces acting from the direction of the chamber end face on the entering streams in a coordinate system rotating with the wave. Then the energy flux through region 1 is written in the form

$$\rho_1 v_1 \left( I_1 + \frac{v_1^2}{2} \right) \delta h = G_1 \left( I_T + \frac{D^2}{2} + \bar{u}_{0x} D \right) + \kappa \rho_2 v_2 \left( I_2 + \frac{v_2^2}{2} \right) h \delta.$$

With consideration of Eqs. (2), (3),

$$\frac{D^2}{v_2^2} + \frac{2I_T}{v_2^2} + \frac{2\bar{u}_{0x}D}{v_2^2} = \frac{\gamma+1}{\gamma-1}. \quad (7)$$

Here  $I_T$  is the total braking enthalpy of the entering mixture;  $D$  is the wave velocity relative to the chamber in the  $x$  direction. Dilution of the flow ahead of the wave by burned up products of the preceding wave does not change the form of the energy equation, due the stationary nature of the flow and its periodicity in  $x$ .

The stationary flow parameters in the chamber section (quantities without numeric subscripts), the pressure  $p_c$ , and the specific momentum  $J$  are independent of the internal flow in the chamber in view of Eq. (1), and are completely determined by the parameters of the injected gas and the geometry by means of the equations

$$v_x = \bar{u}_{0x}, \quad v_z = \sqrt{\frac{\gamma-1}{\gamma+1}} \sqrt{2I_T - \bar{u}_{0x}^2}, \quad (8)$$

$$\rho = \frac{G_1}{\delta l v_z}, \quad p = \frac{G_1 v_z}{\gamma \delta l}, \quad p_c = \frac{G_1}{\delta l} \left( \frac{\gamma+1}{\gamma} v_z - \bar{u}_{0z} \right),$$

$$J = \delta l \frac{p + \rho v_z^2}{G_1} = \frac{1}{\gamma} \sqrt{2(\gamma^2-1)I_T} \sqrt{1 - \frac{\bar{u}_{0x}^2}{2I_T}},$$

which follow from the laws of mass flux, energy, and momentum component conservation.

In contrast to that of [8], the mathematical flow model presented here considers the finite value of the angle of inclination of the wave  $\theta_1$  to the  $z$  axis, which, as is evident from the photographs of Fig. 2, comprises  $\sim 10^\circ$ . This fact is more important for chambers without nozzle narrowing, as are being considered here.

From Eqs. (2), (3), (5)-(8) we obtain a system of equations for calculation of the transverse detonation wave parameters:

$$\zeta + (1 + \gamma - \zeta) \eta \sin \theta_1 - \eta \sqrt{\gamma^2 - 1} \cdot \left[ \frac{\gamma+1}{\gamma-1} - \left( 1 + \frac{1 - \alpha_\zeta^2}{\gamma} \right) \cos^2 \theta_1 \right]^{0.5} = 0,$$

$$\frac{2I_T}{v_2^2} \left( 1 - \frac{\bar{u}_{0x}^2}{2I_T} \right) = \frac{\gamma+1}{\gamma-1} - \left( 1 + \frac{1 - \alpha_\zeta^2}{\gamma} \right) \cos^2 \theta_1,$$

$$\rho_2 = \frac{G_1}{\eta \delta l v_2}, \quad p_2 = \frac{G_1 v_2}{\gamma \eta \delta l}, \quad \frac{p_1}{p_2} = 1 - \gamma \sqrt{\frac{\gamma-1}{\gamma+1} \frac{2I_T}{v_2^2} \frac{H_1}{I_T}}, \quad (9)$$

$$\frac{D}{v_2} = \frac{\gamma+1 - \alpha_\zeta^2}{\gamma} \cos \theta_1 - \frac{\bar{u}_{0x}}{v_2}, \quad \frac{u_{1x}}{v_2} = \frac{\alpha_\zeta^2 - p_1/p_2}{\gamma} \cos \theta_1,$$

$$\frac{v_1}{v_2} = \frac{\rho_2}{\rho_1} = \frac{\gamma+1 - p_1/p_2}{\gamma},$$

where  $\zeta = p_z/p_2$ ;  $\eta = h_1/l$ .

TABLE 2

$\gamma$	$\eta$	$\frac{\sin \theta_1}{\eta}$	$\alpha$	$\frac{p}{p_2}$	$\frac{p}{p_2}$	$\theta, \text{deg}$	$\zeta$	$\frac{D}{v_2}$	$\frac{v_2}{\sqrt{2I_T}}$	$\frac{p_C}{p_2}$
1,15	0,15	1	1	0,1663	0,1353	28,5	0,2480	1,635	0,293	0,2909
	0,15	2	0,5	0,1679	0,1340	27,4	0,2004	1,700	0,296	0,2881
	0,1	2	0,5	0,1131	0,0884	26,3	0,1501	1,768	0,299	0,1901
	0,05	2	0,5	0,0570	0,0438	25,4	0,0839	1,824	0,301	0,0942
1,25	0,2	1	1	0,2320	0,1724	29,3	0,3100	1,521	0,387	0,3879
	0,15	1	1	0,1768	0,1272	28,1	0,2411	1,589	0,393	0,2862
	0,15	1	0,5	0,1814	0,1240	26,1	0,2337	1,687	0,403	0,2791
	0,15	2	0,5	0,1794	0,1254	26,6	0,1895	1,645	0,390	0,2822
	0,1	1	1	0,1200	0,0833	26,4	0,1666	1,658	0,400	0,1875
	0,1	2	0,5	0,1216	0,0822	25,4	0,1428	1,709	0,405	0,1850
	0,05	2	0,5	0,0617	0,0405	24,4	0,0803	1,739	0,412	0,0911
1,667	0,1	2	0,5	0,1556	0,0643	22,5	0,1204	1,532	0,778	0,1714

The auxiliary variable  $\zeta$  is found by solving the first equation of system (9), and subsequently calculating  $v_2$  and all the remaining quantities, if the parameters  $\eta$ ,  $\alpha$ ,  $\theta_1$  and  $H_1/I_T$  are chosen from some additional considerations. We consider the quantities  $I_T$ ,  $\gamma$ ,  $\bar{u}_{0x}$ ,  $\bar{u}_{0z}$ ,  $G_1/\delta l = G/2\pi R\delta$  as specified;  $H_1/I_T$  is determined by the degree of burnup and dilution of the mixture by products before entry into the wave. With the reference chosen for enthalpy calculation, the initial fuel enthalpy is close to the fuel's enthalpy of formation  $H_0$ , so that  $H_1/I_T \approx H_1/H_0 \approx 1 - \kappa$ .

Some results of calculations in which the quantities  $\gamma$ ,  $\eta$ ,  $\sin \theta_1/\eta$  and  $\alpha$  were treated as parameters subject to variation are shown in Table 2. The pressure ratio at the transverse wave  $p_1/p_2$ , in terms of which  $v_1/v_2$  and  $u_{1x}/v_2$  are determined, proves to be weakly dependent on these parameters, and for  $H_1/H_0 < 0.95$  this ratio may be expressed to an accuracy of 10% for all stoichiometric hydrocarbon-oxygen gas mixtures by the formula

$$p_1/p_2 = 1 - 0.97\sqrt{H_1/H_0} \quad (10)$$

The calculated values of the transverse detonation wave velocity  $D$  are close to the detonation speed of an immobile mixture under standard conditions, since  $\cos \theta_1 \approx 1$ , and the incident velocity of the fuel mixture  $u_{1x}$  at  $\bar{u}_{0x} = 0$  proves to be always less than 100 m/sec. The relative pressure amplitude in the wave, characterized by the ratio  $p_2/p_C$ , increases rapidly with decrease in the main geometric parameter of the process  $\eta$ ; the effect of the remaining parameters, except  $\gamma$ , is weaker.

The quantities  $\eta$  and  $\alpha$  can be calculated by supplementing Eq. (9) by Eq. (4). Although exact calculation of the integrals in Eq. (4) is impossible without a detailed calculation of the entire flow field (i.e., a numerical solution of the entire problem), an approximate approach may be used. A series of calculations were performed with various model laws of flow expansion behind the transverse wave. The line  $MC'$  was specified either as straight (in which case  $\alpha = 1$ ,  $\sin \theta_1/\eta = 1$ ) or as an arc of a circle, parallel to the  $x$  axis at point  $M$  and perpendicular to the wave at point  $C$  (in which case  $\sin \theta_1/\eta \approx 2$ ). The flow of detonation products in the vicinity of the line  $MC'$  was considered isentropic, with the change in pressure specified by either the condition  $\rho_2 v_2 / \rho v = 1 + K_1 x$ , corresponding to flow from a cylindrical source with a sonic line on its surface (near  $MC'$  the angle  $\theta$  can be considered small), or by the condition  $\rho_2 v_2 / \rho v = 1 + x/[K_2 x + \eta l / (\theta_1 + \Delta \theta_{13})]$ , where  $\Delta \theta_{13}$  is the angle between the directions  $MC'$  and  $C'E'$  in the vicinity of the point  $C'$ , determined by matching the flow in the centralized rarefaction wave and that behind the oblique shock wave. The constants  $K_1$  and  $K_2$  were chosen such that the pressure in the segment  $x \in (0; l)$  changes from  $p_2$  to a level  $p_1$ , which can be specified independently in accordance with Eq. (10). The second condition obviously produces an elevated value for the derivative  $dp/dx$  along  $MC'$ , while the first produces a lowered value.

The calculation results produced a relationship between  $\eta$  and  $p_1/p_2$ , an approximate expression for which can be written at  $\gamma = 1.25$  in the form

$$p_1/p_2 = 0.45\eta + \eta^2 \quad (11)$$

With the various assumptions as to the flow between the transverse waves enumerated above, the values of  $\eta$  differ from that given by the formula by  $\pm 25\%$  in the range  $\eta \leq 0.2$ , with the smaller values being obtained when an abrupt pressure drop behind the wave is assumed.

Under real conditions the fraction of uncombusted fuel in the mixture ahead of the wave  $H_1/H_0$  is also related to  $\eta$ , since with decrease in  $\eta$  at fixed  $l$  the transverse section of the flow ahead of the wave decreases,



and as a consequence, there is increased dilution by burning products and burnup. Decrease in  $H_1/H_0$ , according to Eqs. (10), (11), leads to growth in  $p_1/p_2$  and  $\eta$ . Thus when  $\eta$  is too small, the process proves impossible. With decrease in  $H_1/H_0$  the temperature ahead of the wave increases, but cannot be above 1200-1500°K because of self-ignition. This limiting temperature corresponds to  $(H_1/H_0)_{\min} \in (0.8; 0.75)$  and  $\eta_{\max} \in (0.2; 0.25)$ . The specification of one additional functional relationship between  $H_1/H_0$  and  $\eta$ , stemming from the mixing and combustion laws for the mixture ahead of the wave, closes system (9)-(11) and permits calculation of all process parameters except the number of waves  $n$ , of which the flow is independent within the framework of the model considered. The number  $n$  can be found only by calculations with more complex models which consider the internal nonsimultaneous structure of the flow within the front.

Actual values of  $h/L$ , measured from the photographs obtained, lie within the interval 0.15-0.22. Taking  $\kappa \approx 0.1$ , we obtain  $\eta \in (0.135; 0.2)$ , which corresponds, according to Eq. (11), to ratios  $p_1/p_2 \in (0.09; 0.14)$  and, according to Eq. (10), to  $H_1/H_0 \in (0.9; 0.8)$ . The lower value of  $H_1/H_0$  and the maximum  $\eta$  agree with the estimate presented above.

The experimentally obtained transverse detonation wave velocities are lower than the calculated values by 10-30%, which may be explained by the nonideal nature of the detonation, caused by the proximity of the actual detonating fuel layer thickness  $h$  to the critical value for a self-supporting process.

On the basis of the studies performed, the following conclusions may be made.

1. Continuous regimes of gas mixture combustion have been obtained in cylindrical ring chambers in the form of transverse detonation waves with a structure similar to that of spin detonation in a circular tube.
2. The range of ring channel geometric parameters over which the detonation combustion regime exists has been studied.
3. A reduction in transverse wave intensity upon narrowing of the ring channel output section has been observed.
4. A flow model has been developed which permits calculation of the basic parameters of the flow with transverse detonation waves in a circular chamber.

#### LITERATURE CITED

1. B. V. Voitsekhovskii, Dokl. Akad. Nauk SSSR, 129, No. 6 (1959).
2. B. V. Voitsekhovskii, Zh. Prikl. Mekh. Tekh. Fiz., No. 3 (1960).
3. V. V. Mikhailov and M. E. Topchiyan, Fiz. Goreniya Vzryva, 1, No. 4 (1965).
4. F. A. Bykovskii, I. D. Klopotov, and V. V. Mitrofanov, Dokl. Akad. Nauk SSSR, 224, No. 5 (1975).
5. B. V. Voitsekhovskii, V. V. Mitrofanov, and M. E. Topchiyan, Detonation Front Structure in Gases [in Russian], Izd. SO Akad. Nauk SSSR, Novosibirsk (1963).
6. V. V. Mitrofanov and V. A. Subbotin, in: Combustion and Explosion [in Russian], Nauka, Moscow (1977).
7. Brian and Edwards, Sixteenth Symposium (International) on Combustion, Pittsburgh (1976).
8. P. I. Shen and T. C. Adamson, Astron. Acta, 17, 715 (1972).